

A GLOBAL ASSESSMENT OF HISTORICAL AND FUTURE TSUNAMI HAZARDS BASED ON SEISMIC RECORDS OVER THE LAST 400 YEARS AND ESTIMATED SEISMIC GAPS

**WORLD
TSUNAMI
AWARENESS
5 NOVEMBER
2017 DAY**



**TOHOKU
UNIVERSITY**



IRIDeS
International Research Institute
of Disaster Science
災害科学国際研究所

Contributors:



Japan Asia Group

KOKUSAI KOGYO



esri Japan



**TOKIOMARINE
NICHIDO**

Willis Research Network

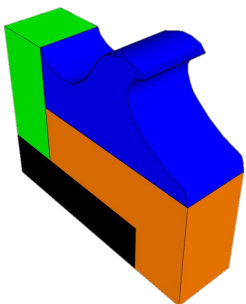
A GLOBAL ASSESSMENT OF HISTORICAL AND FUTURE TSUNAMI HAZARDS

BASED ON SEISMIC RECORDS OVER THE LAST 400 YEARS AND ESTIMATED SEISMIC GAPS

Prepared by
Fumihiko Imamura
Anawat Suppasri
Panon Latcharote
Takuro Otake
Natt Leelawat
David N. Nguyen

International Research Institute of Disaster Science (IRIDeS)
Tohoku University

Contributors:
Kokusaikogyo Co., Ltd.,
Esri Japan Corporation,
Tokio Marine & Nichido Fire Insurance Co., Ltd., and
Willis Research Network



Second Updated on 5 November 2017
First Updated on 27 December 2016
First published on 31 October 2016

Executive Summary

This report is our contribution towards World Tsunami Awareness Day, which was proposed by the United Nations (UN) in 2015. We conducted a global tsunami hazard assessment for local regions, including low tsunami risk areas, based on a 400-year database which allows insight on past and potential future tsunamis based on the seismic gap.

The resulting tsunami hazard could be displayed on a global map and enables us to easily observe the local effects of tsunamis. Two criteria were selected to represent the past 100 major earthquake generated tsunamis: First, the earthquakes must be larger than magnitude 7.5 and secondly, occurred after the year 1600. A total of 18 events were chosen from locations within the seismic gap and selected based on asperities found in large subduction zones characterized by Lay et al. (1982). The earthquake magnitude was then determined by the length of the seismic gap that are no larger than nearby maximum past events. Based on the results of the simulation, the locations of modern tsunamis (from the periods of 1970 to 2016) are greater than 2 meters in height, and limited to areas affected by the 2004 Indian Ocean Tsunami and the 2011 Great East Japan Tsunami. Regardless, damaging tsunamis have been witnessed everywhere in the world, especially along the Pacific Rim. This observation demonstrates the importance of assessing and understanding the hazards based on historical events. Potential tsunamis from the seismic gap demonstrated the importance of simultaneously assessing both local and distant tsunamis. For example, we have demonstrated that New Zealand is potentially vulnerable to locally generated tsunamis despite past records being exclusively limited to tsunamis generated from distant locations. Comparisons between tsunami height and wave force show that only using the tsunami height might underestimate building damage. We wish that as a part of the World Tsunami Awareness Day related activities, our results and findings will increase tsunami awareness at the global scale, especially in comparatively low tsunami risk areas, and reduce human loss from future tsunamis.

1. Purpose

A tsunami is classified as a low-frequency, and high-impact natural hazard. Reducing tsunami vulnerabilities, managing risks, and limiting its effects based on global scientific assessments can be difficult due to the lack of information and experiences. While high tsunami risk regions such as the Pacific and Indian Oceans have implemented countermeasures based on lessons and experiences from the past, much fewer measures have been adopted in low-risk areas. In such cases, although the risk of a tsunami is less likely than high risk areas, unknown risks continue to persist and the potential for even small tsunamis to cause catastrophic damages also exist. Once a tsunami is generated from a seismic fault or landslide, the wave can propagate across entire oceans and affect many countries (*United Nations International Strategy for Disaster Reduction (UNISDR), 2009; Løvholt et. al, 2012*). This phenomenon is why international collaboration with networks for tsunami mitigation is essential. We can properly evacuate people and save lives by using the available time before a tsunami arrives after its initial propagation across the ocean. In other words, knowledge and information can save lives from the threat of tsunamis, including the possibility of achieving zero fatalities with proper preparation.

**WORLD
TSUNAMI
AWARENESS
DAY**
5 NOVEMBER
2017



We wish to contribute to **World Tsunami Awareness Day**, which was proposed by the United Nations in 2015, by conducting a global tsunami hazard assessment for local regions that are based on a 400 year data base of historical tsunamis. Stakeholders can better anticipate future tsunamis based on seismic gaps, while the resulting tsunami hazard data can be displayed on an atlas that will easily enable users to observe the local effects of tsunamis.

2. Major Earthquake-Generated Tsunami in the Last 400 Years

Within a roughly 10 year period between the 1950s to 1960s, three devastating tsunamis were generated by earthquakes that were magnitude (M_w) 9.0 or larger (*Tsunami Laboratory, 2016*). All of them were located along the Pacific Rim. The 1952 Kamchaka earthquake (9.0 M_w) generated large tsunamis that caused catastrophic damages and human loss around the Kamchatka Peninsula and the Kuril Islands, while Hawaii received property damages but no human casualties, and no damages and casualties in Japan (*Johnson & Satake, 1999*). The 1960 Chilean Tsunami was generated by a (9.5 M_w) (9.5 M_w) earthquake, the largest ever instrumentally recorded, causing widespread damages and fatalities due to the accompanying transoceanic tsunami that also impacted Hawaii and Japan (*Fujii & Satake, 2013*). The 1964 Alaskan Earthquake (9.2 M_w) is the second largest observed Earthquake (*Ichinone et al., 2007*). Its associated tsunami hit a large part of southern Alaska and neighboring areas of the western Canada and the West Coast of US but with minor damage and no fatalities to Hawaii. After the end of this series of devastating tsunamis, other major tsunamis such as the 2011 Great East Japan tsunami were occurred along the Pacific Rim with the exception of the 2004 Indian Ocean tsunami.

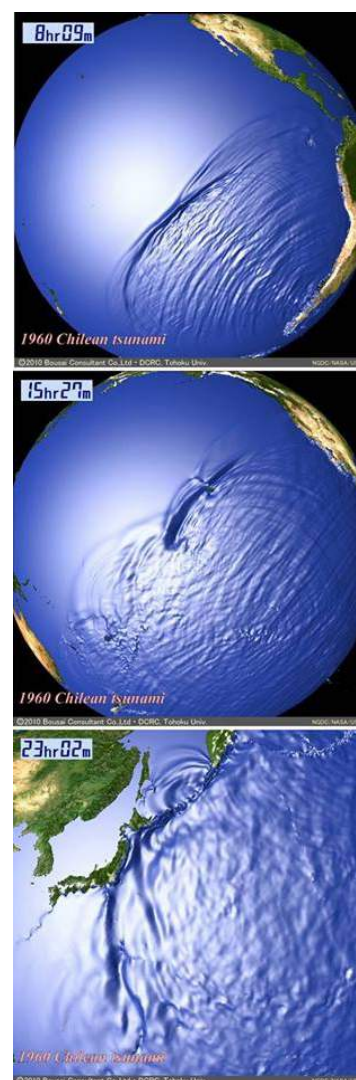


Figure 1

Simulation of the 1960 Chilean tsunami

Although the Pacific Ocean is considered the most tsunami prone region in the world, information on historical tsunamis exist in even low tsunami risk areas such as the Atlantic Ocean, the Mediterranean Sea, the Black Sea, the Caribbean Sea, and the western United States. For example, the 1700 Cascadia earthquake occurred along the west coast of the US with the estimated magnitude of 9.0 M_w . A Large transoceanic tsunami followed the earthquake and struck the west coast of the US and Canada. The tsunami also hit the coast of Japan based on Japanese records, noting that the wave was not tied to any other Pacific Rim earthquake. Within Europe, the 1755 Lisbon Tsunami was one of the most catastrophic events that had ever occurred in Atlantic Ocean and devastated Europe, particularly in modern-day Portugal, Spain and Morocco, with waves observed in Ireland and the Lesser Antilles (Santos *et al.*, 2009).

The tsunami caused severe damages and a large number of casualties as high as 60,000. (Tsunami Alarm System, 2016a). In the Mediterranean Sea, it is said that a disastrous tsunami takes place in this region on average, every century, based on a long record of historical tsunamis since 1628 BC (Tsunami Alarm System, 2016b). Greece, Turkey and southern Italy are the most tsunami affected countries in the region. There are some major tsunamis such as local tsunamis that damaged southern Italy in 1905 and 1907, another tsunami that affected Cyclades and Dodecanese Islands, Crete, and the Turkish coast of Asia Minor. In 1956 (Okal *et al.*, 2009), and a local tsunami within the enclosed Sea of Marmara in 1999 (Latcharote *et al.*, 2016) led to an estimated 17,000 fatalities (Tsunami Alarm System, 2016b; Piatanesi & Tinti, 2002).

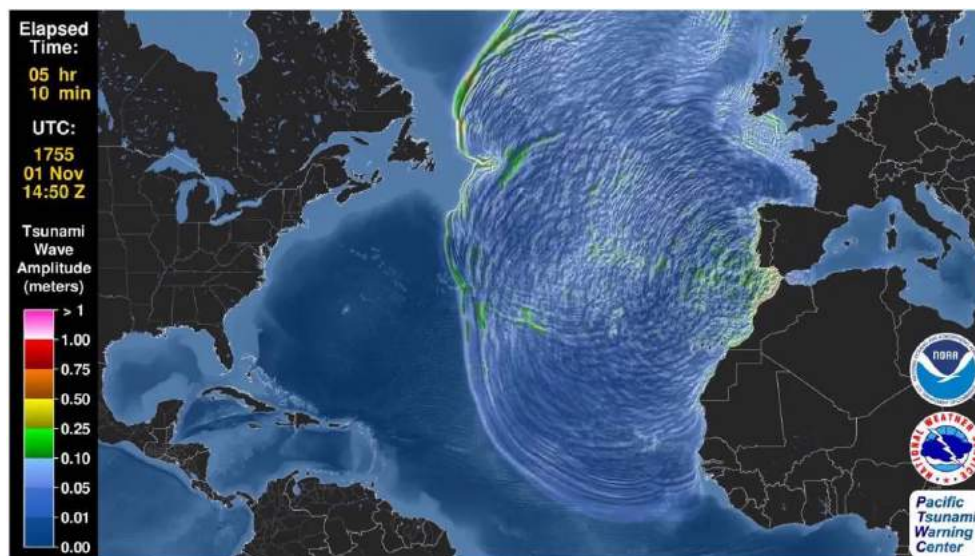


Figure 2

Simulation of the 1755 Lisbon tsunami

Note. Source: *Tsunami forecast model animation of 1 November 1755 Lisbon, Portugal tsunami*, by D. Wang, & N. Becker, 2015.

3. Selection of Seismic Events

100 major historical earthquake-generated tsunamis were selected to represent tsunami hazards on a global scale. These 100 events were selected from a total of 17 tsunami source regions from a global historical tsunami database (*National Geophysical Data Center/World Data Service (NGDC/WDS), 2016*). Two main criteria were used for the event selection.

First, the earthquake magnitude must be larger than 7.5, which is the general condition for earthquake-induced tsunamis. Since the first criterion relies on the magnitude of the earthquake regardless of fault mechanism, some events exist where a large magnitude earthquake occurred but generated a small tsunami due to a strike-slip fault mechanism.

In addition, seismic events that produced landslides occurred, however most of the fault parameters only represent seismic sources. Only the 1771 Meiwa Tsunami which had a landslide source, was represented as a seismic source for the sake of convenience.

Secondly seismic events after 1600 were selected due to the return period of large earthquakes is generally greater than 300-400 years. Seismic gap regions will be considered in future research.

Seismic Gap

A seismic gap as defined by the U.S. Geological Survey (*USGS, 2016*) as a section of a fault that has produced earthquakes in the past but is now dormant.

For some seismic gaps, no earthquakes have been observed historically, but it is believed that the fault segment is capable of producing earthquakes on some other basis, such as plate-motion information or strain measurements.

In addition to the selected 103 past events, 18 potential major events generated in the seismic gap were determined based on asperities found in large subduction zones in the Pacific Ocean categorized by Lay et al. (1982). The earthquake magnitude was determined by the length of the seismic gap but not larger than the maximum past event nearby. Other fault dimensions were calculated using an empirical relationship with earthquake magnitude which will be explained in the later section. Other fault mechanisms related information was considered from past events.

4. List of Earthquake Events and Its Distributions

Table 1 List of earthquake induced tsunami events

No.	Year	M	Location	Lat.	Lon.	Max. Water Height (m)	Deaths	Damage (\$Mill.)	House Destroyed
1	1677	8.0	Boso	35.000	142.000				
2	1687	8.5	S Peru	1.000	-81.500	5.0	1,000		
3	1692	7.7	Jamaica	17.800	-76.700	1.8	2,000		
4	1700	9.0	Cascadia Subduction Zone	-13.500	-75.500		5,000		
5	1703	8.2	Off SW Boso Peninsula	34.700	139.800	10.5	5,233		20,162
6	1707	8.4	Nankaido	33.200	134.800	25.7	5,000		17,000
7	1730	8.7	Central Chile	-28.550	-70.760	9.0	200		
8	1755	8.5	Lisbon (Portugal)	37.000	-10.000	18.3	50,000		
9	1762	8.8	Arakan	21.000	89.000	1.8			
10	1771	7.5	Ishigaki Is (Meiwa)	24.000	124.600				
11	1787	8.3	San Marcos	45.000	-125.00		2		
12	1788	8.0	Alaskan Peninsula	57.000	-153.000	30.0			
13	1812	7.5	S California	-32.500	-71.50				
14	1819	8.5	N Chile	-27.000	-71.50				
15	1833	8.3	SW Sumatra	-2.500	100.500				
16	1837	8.5	S Chile	19.500	-104.300	10.0	4		
17	1842	8.1	Haiti	19.750	-72.200	5.0	300		
18	1843	8.3	Guadeloupe (French Territory)	16.500	-62.200	1.2			
19	1852	8.3	Banda Sea	-5.250	129.750	8.0	60		
20	1854	8.3	Enshunada Sea	34.000	137.900	21.0	300		8,300
21	1865	8.0	Tonga Is	-19.500	-173.500	1.3			20
22	1868	7.6	New Zealand	-40.200	173.000				
23	1868	7.9	Hawaii	19.000	-155.500	13.7	47		108

No.	Year	M	Location	Lat.	Lon.	Max. Water Height (m)	Deaths	Damage (\$Mill.)	House Destroyed
24	1868	8.5	S Peru	53.600	-133.300	0.61			
25	1877	8.3	N Chile	-38.140	-73.410	25.0	2,223	1,000	58,622
26	1882	7.9	Panama	10.000	-79.000	3.0			
27	1886	7.7	Charleston (USA)	32.900	-80.000				
28	1889	8.0	N Moluccas Is	1.000	126.250	4.0			
29	1897	8.7	Sulu Sea	6.000	122.000	7.0	13		33
30	1899	8.2	Yakutat Bay	60.000	-140.000	61.0			
31	1905	7.9	Italy	39.000	16.000	1.3			
32	1906	8.8	Off Coastal Ecuador	16.300	-95.800	0.4			
33	1911	8.0	Ryukyu Is	28.000	130.000				
34	1917	8.0	Kermadec Is	-29.200	-177.000	0.3			
35	1917	8.3	Samoa Is	-15.500	-173.000	12.2			
36	1918	8.3	Celebes Sea	5.500	123.000	7.2	6		
37	1918	8.2	S Kuril Is	45.500	151.500	12.0	23		2
38	1919	8.1	Tonga Is	-18.352	-172.515	2.5			
39	1922	8.7	N Chile	18.19	-102.53	3.0			
40	1924	8.3	E Mindanao Is	6.500	126.500				
41	1932	8.1	Central Mexico	16.500	-98.500	4.0	11		
42	1933	8.4	Sanriku	39.224	144.622	29.0	3,022		6,000
43	1934	7.9	South China Sea	17.500	119.000				
44	1938	8.2	Shumagin Is	55.48	-158.37				
45	1938	8.5	Banda Sea	-5.250	130.500	3.4			24
46	1939	7.7	S Black Sea (Turkey)	39.770	39.533	0.5			
47	1941	8.3	Azores Gibraltar Fracture Zone	37.417	-18.983	0.1			
48	1941	7.6	Andaman Sea, E Coast of India	12.500	92.500	1.5			
49	1945	8.0	Makran Coast	24.500	63.000	17.0	4,000	25	
50	1946	8.6	Aleutian	53.492	-162.832	42.0	167	24	
51	1948	8.3	Sulu Sea	10.500	122.000				
52	1948	7.8	Tonga Trench	-21.000	-174.000	2.0			
53	1949	8.1	British Columbia	34.200	-119.900	3.4			
54	1952	7.8	E of Mindanao Is	9.500	127.250				

No.	Year	M	Location	Lat.	Lon.	Max. Water Height (m)	Deaths	Damage (\$Mill.)	House Destroyed
55	1952	8.1	Tokachi	42.150	143.850	6.5	33		
56	1952	9.0	Kamchatka	52.755	160.057	18.4	10,000	1	
57	1956	7.8	Greece	36.900	26.000	30.0	3		
58	1957	8.6	Andoreanof Is	51.290	-175.630				
59	1960	9.5	S Chile	11.730	-87.390	9.9	170	30	1,500
60	1964	9.2	Alaska	61.017	-147.648	67.1	124	116	
61	1964	7.5	NW Honshu Is	38.650	139.200	5.8	26	80	1,960
62	1965	8.7	Rat Is and Aleutian Is	51.300	178.600	10.7		0.1	
63	1965	7.8	Mexico	-42.50	-74.000	6.0	16		
64	1969	7.7	Kamchatka	57.700	163.600	15.0			
65	1973	7.5	Quezon (Philippines)	13.400	122.800	1.3			
66	1974	8.1	Central Peru	-12.270	-77.790				
67	1975	7.6	Philippine Trench	12.540	125.993	3.0			30
68	1975	7.9	Solomon Sea	-6.590	155.054	2.0			
69	1976	8.0	Moro Gulf	6.292	124.090	9.0	6,800	134	
70	1977	8.0	Sunda Is	-11.085	118.464	15.0	189	1	
71	1977	8.1	Solomon Is	-9.965	160.731	0.04			
72	1980	7.7	Algeria	36.195	1.354	0.7			
73	1981	7.6	New Zealand	-48.790	164.360				
74	1983	7.8	Noshiro	40.462	139.102	14.9	100	800	3,513
75	1985	8.0	Mexico	-18.600	-71.000	18	25,000		
76	1986	7.8	Taiwan	23.901	121.574	0.3			
77	1990	7.5	Mariana Trench, N Mariana Is	15.125	147.596	1.8			
78	1992	7.8	Flores Sea	-8.480	121.896	26.2	1,169	100	31,785
79	1992	7.7	Nicaragua	-21.500	-70.500	24.0	2,282		
80	1993	7.7	Sea of Japan	42.851	139.197	32.0	208	1,207	2,374
81	1994	7.8	South of Java	-10.48	112.84				
82	1994	8.3	S Kuril Is	43.773	147.321	10.4			2
83	1996	7.9	Sulawesi	0.729	119.931	7.7	9	1	400
84	1996	8.2	Irian Jaya	-0.891	136.952		110	4	
85	1996	7.5	N Peru	-9.593	-79.587	5.1	12		15

No.	Year	M	Location	Lat.	Lon.	Max. Water Height (m)	Deaths	Damage (\$Mill.)	House Destroyed
86	1997	7.7	Santa Cruz Is, Vanuatu	-12.584	166.676	3.0			7
87	1997	7.8	Kamchatka	54.841	162.035	8.0			
88	1999	7.6	Turkey	40.760	29.970	2.5	155		
89	1999	7.5	Vanuatu Is	-16.423	168.214	6.6	5		
90	2000	7.6	Sulawesi	-1.105	123.573	6.0			
91	2000	8.0	New Ireland	-3.980	152.169	3.0			
92	2001	8.4	S Peru	-16.265	-73.641	8.8	26		2,000
93	2002	7.6	Bismarck Sea	-3.302	142.945	5.5			
94	2004	9.1	Off W Coast of Sumatra	3.316	95.854	50.9	227,899	10,000	
95	2004	8.1	Macquarie Is	-49.312	161.345	0.3			
96	2005	8.7	Nias	2.085	97.108	4.2	10		
97	2006	7.7	S Java	-9.254	107.411	20.9	802	55	1,623
98	2006	8.3	S Kuril Is	46.592	153.266	21.9			
99	2007	8.1	Solomon Is	-8.460	157.044	12.1	52		2,500
100	2010	8.8	Central Chile	-36.122	-72.898	29.0	156	30,000	
101	2011	9.0	Honshu Is	38.297	142.372	38.9	18,453	220,085	273,796
102	2013	7.9	Santa Cruz Is	-10.766	165.114	11.0	10		588
103	2013	7.8	Scotia Sea (Antarctica)	-60.296	-46.362	0.2			

Table 2 Earthquake fault parameters for the selected 18 potential events in seismic gap

No.	Region	Mw	Lon.	Lat.	Depth	Slip	Dip	Strike	Slip angle	Length	Width
1	Aleutian Is	8.7	169.4	53.5	5.00	6.14	21.77	302.8	90	394	117
2	W Guatemala	8.9	-91.7	14.4	37.48	8.24	23.00	297.6	90	507	135
3	Costa Rica	8.7	-84.4	9.1	5.00	6.14	7.00	296.6	90	394	117
4	Panama	8.7	-80.7	7.6	17.94	6.14	18.00	269.5	90	394	117
5	Columbia	8.7	-77.7	4.5	5.00	6.14	6.00	24.1	90	394	117
6	W Ecuador	8.7	-81.4	-4.3	5.00	6.14	5.33	4.8	90	394	117
7	W Peru	8.6	-80.5	-7.7	56.4	5.30	21.75	335.4	90	347	109

No.	Region	Mw	Lon.	Lat.	Depth	Slip	Dip	Strike	Slip angle	Length	Width
8	E Philippines	8.2	125.9	10.8	7.64	2.94	37.80	155.0	90	209	82
9	NE Philippines	8.2	123.7	15.1	6.38	2.94	23.00	117.6	90	209	82
10	New Zealand	8.3	176.5	-41.4	5.00	3.40	19.56	250.7	90	237	88
11	New Zealand	8.3	178.3	-39.7	5.00	3.40	12.48	196.7	90	237	88
12	New Zealand	8.3	179.4	-37.0	5.00	3.40	17.48	202.2	90	237	88
13	Solomon Is	8.1	149.8	-6.5	5.00	2.54	13.13	260.1	90	184	76
14	Solomon Is	8.1	151.3	-5.9	5.00	2.54	21.88	238.2	90	184	76
15	Vanuatu	8.1	166.6	-15.1	5.00	2.54	28.75	365.6	90	184	76
16	Vanuatu	8.1	167.9	-18.3	5.00	2.54	22.32	348.6	90	184	76
17	New Caledonia	8.1	169.0	-20.6	5.00	2.54	40.25	332.9	90	184	76
18	New Caledonia	8.1	170.1	-22.0	5.00	2.54	20.03	311.9	90	184	76

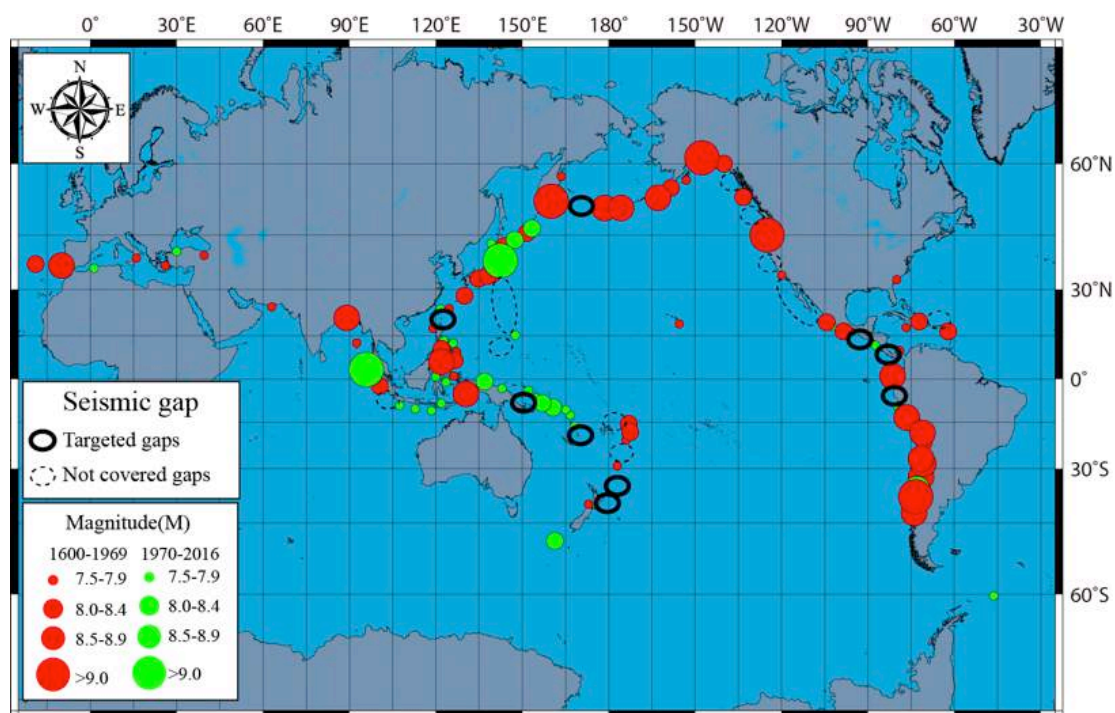


Figure 3

Distributions of the 103 selected past earthquakes and 18 potential earthquakes

Note. Green: 39 events that occurred during 1600 to 2016;

Red: 64 events that occurred during 1600-1969.

The sizes of the circles indicate the earthquake magnitude, which ranges from 7.5 to greater than 9.0 and greater.

The rings represent the gap areas.

5. Earthquake Fault Parameters

Only static fault parameters (rupture velocity was considered to be infinite) were used to calculate seafloor and coastal deformation. Nine fault parameters were required for each earthquake event, namely, the latitude, longitude, focal depth (H), fault length (L), fault width (W), displacement (D), strike angle (θ), dip angle (λ) and rake angle (δ).

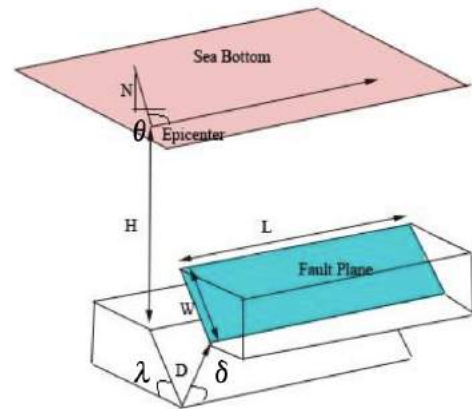


Figure 4

Illustration of earthquake fault parameters

Source: *Tsunami Modelling Manual (TUNAMI model)*, by F. Imamura, A. C. Yalciner, & G. Ozyurt, 2006, p. 15.

$$\text{Fault length, } L \text{ (in km):} \quad \log L = 0.55 M_w - 2.19, 6.7 \leq M_w \leq 9.2 \quad (1)$$

$$\text{Fault width, } W \text{ (in km):} \quad \log W = 0.31 M_w - 0.63, 6.7 \leq M_w \leq 9.2 \quad (2)$$

$$\text{Displacement, } D \text{ (in cm):} \quad \log D = 0.64 M_w - 2.78, 6.7 \leq M_w \leq 9.2 \quad (3)$$

6. Bathymetry and Topography Data

Two main computational regions exist regarding the energy distribution of each tsunami event, namely, the bathymetry and topography, which are focused within 1) the Pacific and Indian Oceans and 2) the Atlantic Ocean.

6.1 The Pacific Ocean and Indian Ocean

Column (x): 4,320
Row (y): 2,160
Cell size: 0.083333333
(5 arc-min, about 10 km)
xllcorner: -25 and yllcorner: -90

A General Bathymetric Chart of the Oceans (GEBCO) 30 arc-sec (approximately 900 m) grid (GEBCO, 2016) was used as the original bathymetry and topography data for the simulation. The data was then resampled to a resolution of 10 km (5 arc-min) to conduct numerical tsunami simulations on a global scale.

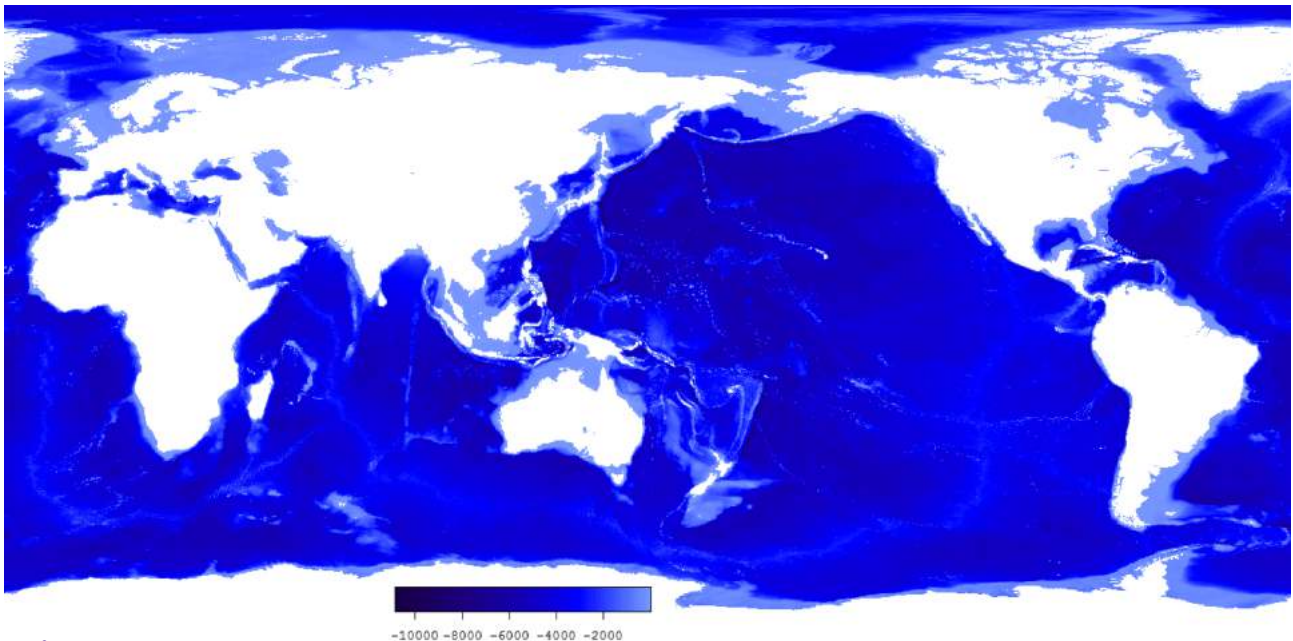


Figure 5

Bathymetry and topographic data from the Pacific Ocean and Indian Ocean

6.2 Atlantic Ocean

Bathymetry and topography data from the Atlantic Ocean were utilized in order to better understand seismic events that caused transoceanic tsunamis across the Atlantic Ocean, particularly those that affected Europe, the eastern coast of the United States, and the Caribbean Sea.

Column (x): 3,240
Row (y): 1,728
Cell size: 0.083333333
(5 arc-min, about 10 km)
xllcorner: -135 and yllcorner: -72

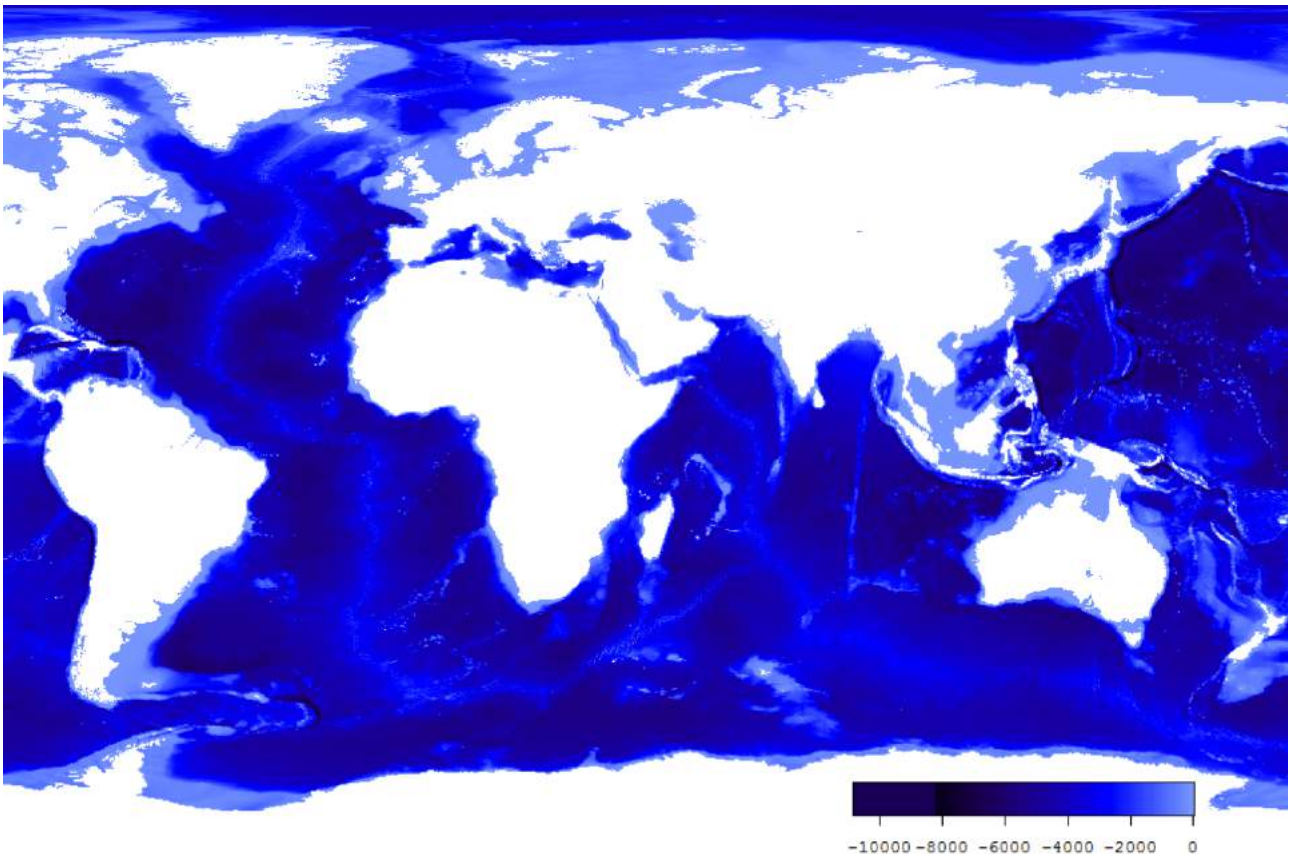


Figure 6

Bathymetry and topographic data from the Atlantic Ocean

7. Tsunami Numerical Simulation

Numerical simulations of distant source tsunamis were conducted by using a code that was developed by Tohoku University, the **Tohoku University's Numerical Analysis Model for the Investigation of Near-field tsunamis (TUNAMI)** (*IUGG/IOC TIME Project, 1997*). This model uses a staggered leap-frog scheme to solve shallow water equations that describe the nonlinear long-wave theory (*Imamura, 1996; Nagano et al., 1991; Suppasri et al., 2010*). These simulations were performed following the fault parameters for each case, as previously shown in Table 1. The initial sea surface conditions were prepared by using formulas to calculate seafloor and coastal deformation from submarine faulting with earthquake fault parameters (*Okada, 1985*). The simulation time was set to 24 h, ensuring that the maximum tsunami height would be obtained and that the tsunami could travel across the oceans. A reflective boundary condition was imposed on the shorelines across the entire area to ignore tsunami inundation along the coast. Therefore, wave amplification in nearshore areas was not considered in these simulations.

Q: What is the earliest possible warning that one can receive before a tsunami hits the shore?

A: Shaking due to a large earthquake can range from one to three minutes and can be considered as a prelude to a tsunami. For distant locations where the shaking could not be felt, national level tsunami warning systems can be disseminated within 3 minutes in Japan (*Suppasri et al., 2016*), about 7 minutes in Thailand (*Leelawat et al., 2015*), and 10 minutes by a regional level system established by the Pacific Tsunami Warning Center (*PTWC, 2016*).

8. Output Image

The simulation outputs consisted of the maximum amplitude, maximum flow velocity, maximum hydrodynamic force and arrival time (for tsunami amplitudes higher than 0.05 m). A visualization of the results (maximum amplitude and arrival time) is shown below.

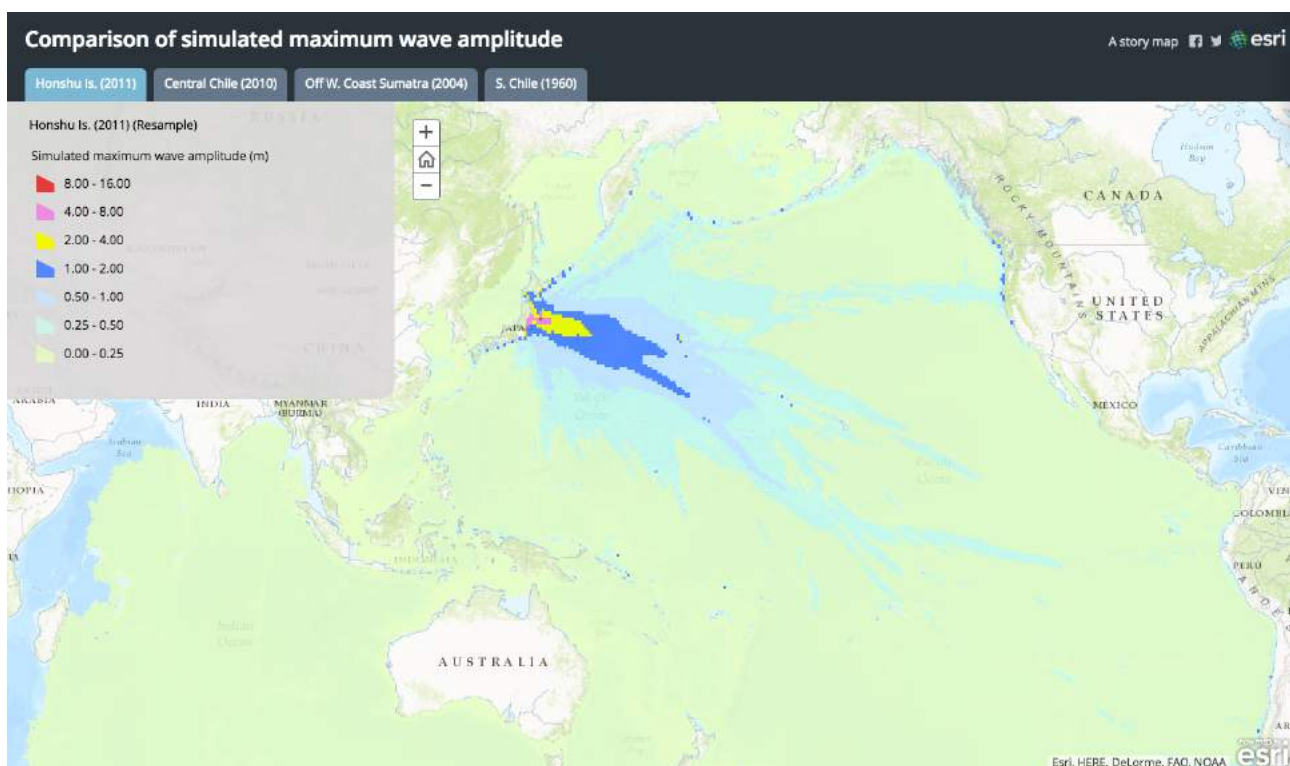


Figure 7

Maximum offshore tsunami amplitude distribution

Note. An example from the 2011 Great East Japan earthquake and tsunami)

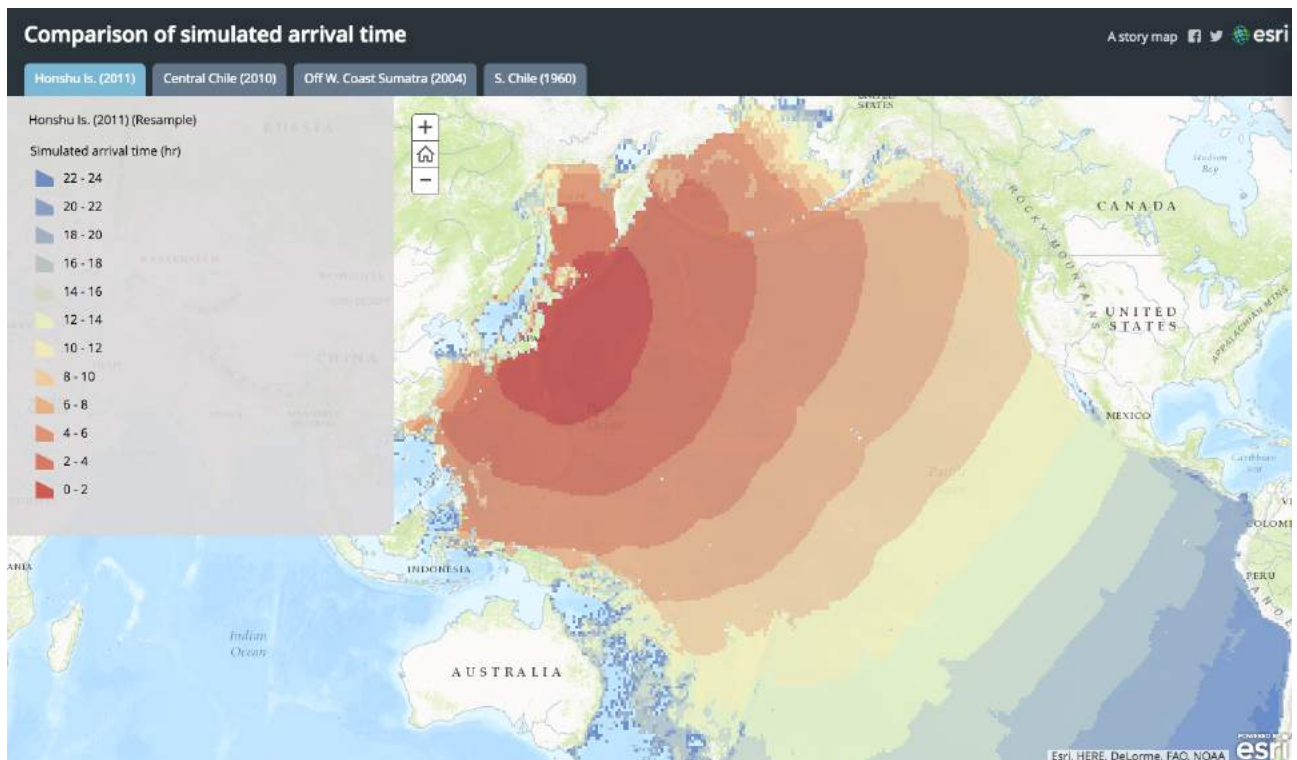


Figure 8

Tsunami arrival time

Note. An example from the 2011 Great East Japan earthquake and tsunami

Q: A What are the factors that influence the tsunami arrival time?

A: The arrival time of tsunami depends on the distance from the tsunami source and sea depth. In the case of the 1993 Hokkaido Earthquake, the first tsunami arrived within 4-5 minutes after the earthquake as the epicenter was very close to the affected area (*National Oceanic and Atmospheric Administration (NOAA), 2016*). Tsunamis can travel as fast as an aircraft in the deep sea and at the speed of a vehicle in shallower areas. In case of the 2004 Indian Ocean Earthquake, the tsunami arrived at Thailand almost simultaneously to its arrival in Sri Lanka. This is because even though the distance from the earthquake to Thailand is shorter, the average sea depth to Thailand is much shallower (*Suppasri et al., 2016*).

9. Discussion

9.1 Gap between Historical and Recent Tsunamis

The memories and traditions of tsunami events can be limited and as a result, a gap between our experiences and historical tsunamis continue to persist. **Figures 9** and **10** display the simulated maximum tsunami amplitude based on 34 and 52 events (excluding the events that affected the Atlantic Ocean) from the periods of 1970-2016 and 1600-1969, respectively. A tsunami amplitude of 2 m was selected as the criterion in this map because the damage from a tsunami significantly increases when the tsunami exceeds 2 m. **Figure 9** displays the locations of tsunamis that exceeded 2 m were mainly located in areas affected by the 2004 Indian Ocean Tsunami and the 2011 Great East Japan Tsunami based on recent experiences (1970-2016). On the other hand, damaging tsunamis that exceeded 2 m was seen virtually everywhere, especially along the Pacific Rim.

Figures 9 and **10** can also be interpreted by using a tsunami intensity scale that was proposed by *Papadopoulos and Imamura (2001)*. The tsunami intensity (*I*) scale (**Table 3**) (twelve grades) is independent of any physical parameters and includes the effects on humans and natural environments and the vulnerability of structures based on recent experiences regarding tsunamis. The tsunami intensity grades I–V refer to small tsunamis, where shaking from the earthquake could not be felt. Intensity grade VI indicates a slightly damaging tsunami. Intensity grades VII–VIII are used to define damaging and heavily damaging tsunamis, whereas grades IX–X refer to destructive and very destructive tsunamis. Finally, intensity grades XI–XII denote devastating and completely devastating tsunamis. The correlation of the maximum tsunami heights for each intensity grade is shown according to a power function of 2, which varies from zero to five (**Table 3**). The color bar of the maximum tsunami amplitude was also set following the tsunami intensity scale to improve visualization (see **Table 3**).

Q: Can the second wave of tsunami be the largest wave?

A: Yes. The second wave can be larger than the first wave as we can see in the 2016 Fukushima tsunami in Japan. Due to the faulty orientation focused the tsunami into Sendai Bay along with the wave reflection and refraction, the second wave observed at Sendai Port was the largest wave for that tsunami (Suppasri et al., 2017).

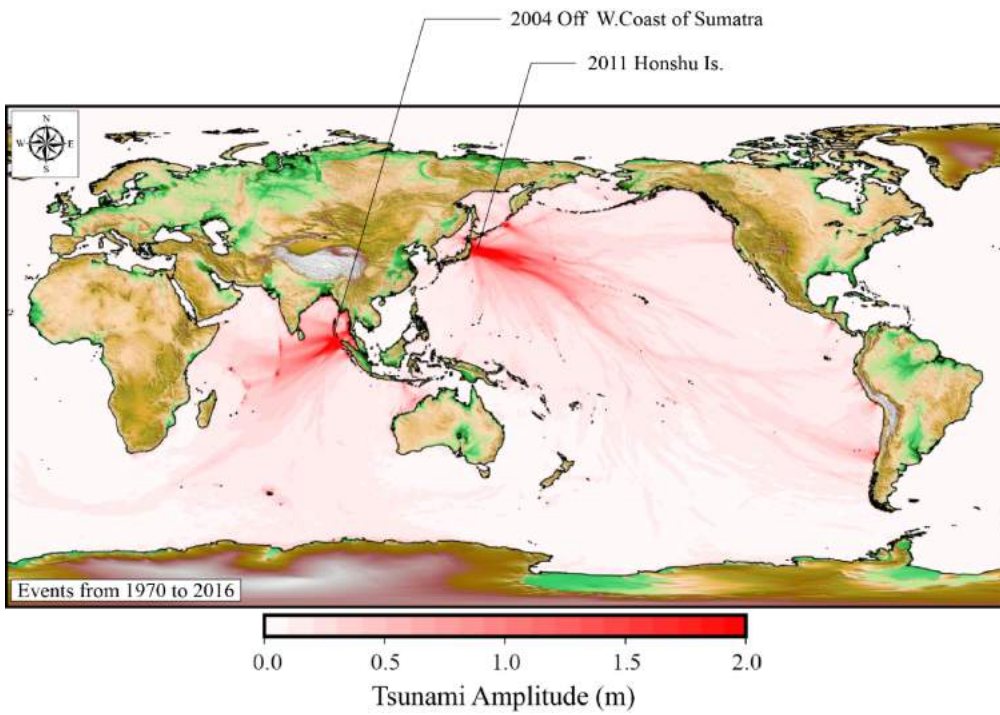


Figure 9

Simulated maximum tsunami amplitude based on events from 1970 to 2016 (Pacific and Indian Oceans)

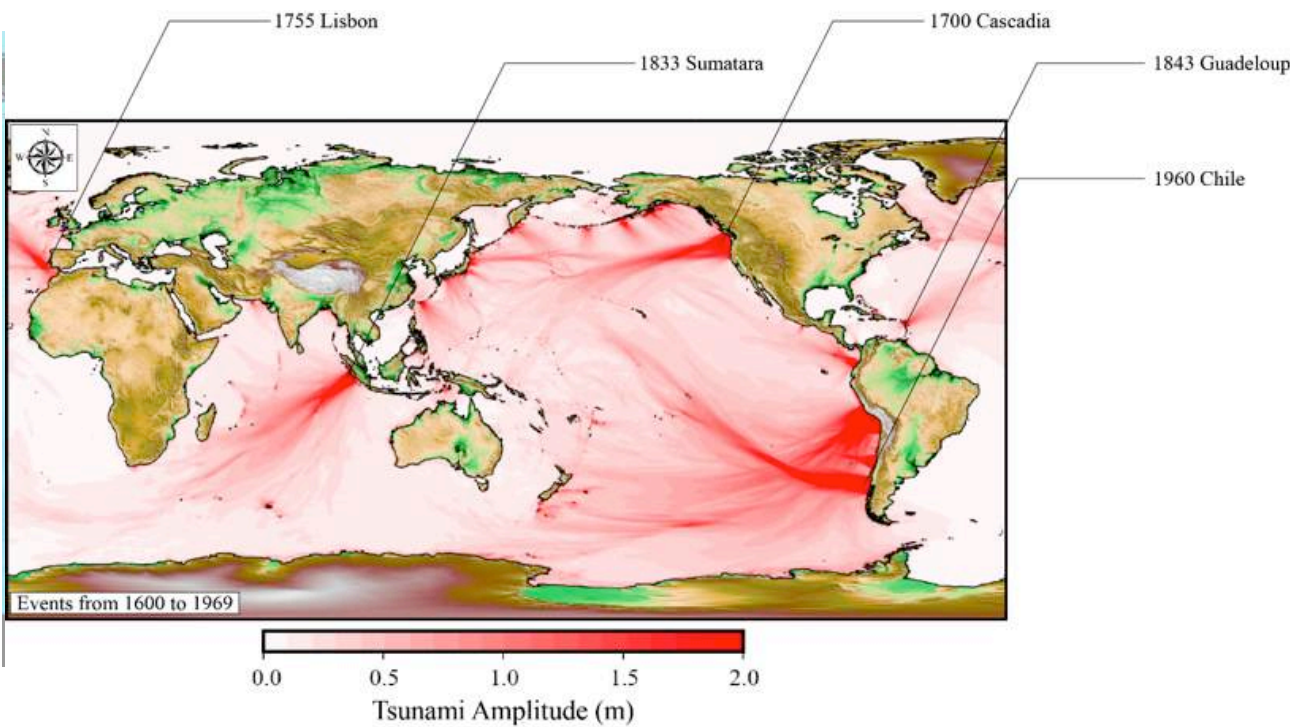


Figure 10

Simulated maximum tsunami amplitude based on events from 1600 to 1969 (Pacific and Indian Oceans)

Table 3 Tsunami intensity and correlated maximum shoreline tsunami amplitude

Intensity (I)	Definition	Max. Shoreline Amplitude	Color Bar
I–V	Not felt (I), Scarcely felt (II), Weak (III), Largely observed (IV) and Strong (IV)	< 1.00 m	0.00 - 0.25 m 0.25 - 0.50 m 0.50 - 1.00 m
VI	Slight damages (VI)	< 2.00 m	1.00 - 2.00 m
VII–VIII	Damages (VII) and Heavy damages (VIII)	< 4.00 m	2.00 - 4.00 m
IX–X	Destructive (IX) and Very destructive (X)	< 8.00 m	4.00 - 8.00 m
XI–XII	Devastating (XI) and Completely devastating (XII)	> 8.00 m	> 8.00 m

Q: How far inland can a tsunami travel?

A: Small tsunamis can be fully or partially mitigated by coastal defense structures such as breakwaters and seawalls. However, large tsunamis such as the ones generated by the 2004 Indian Ocean, can penetrate as far as 1-2 km inland as in the case of, Khao Lak, Thailand (Suppasri et al., 2011), 3-4 km in Banda Aceh, Indonesia (Suppasri et al., 2015), as well as 4-5 km in the Sendai Plains in case of the 2011 Great East Japan tsunami (Suppasri et al.,

9.2 Differences between Tsunami Height and Wave Force

Tsunami height is a typical hazard index applied to tsunamis and most frequently used to understand the characteristics of a tsunami and associated damages. Wave force was selected as the most suitable factor to explain the risk according to recent data of damaged houses, boats and infrastructures. Some examples from two regions are shown to understand the differences between tsunami height and wave force.

The wave force as hydrodynamic force is often calculated by using the drag equation (drag force, F_D), as shown in **equation (4)** below.

$$F_D = 0.5 \times C_d \times \rho \times A \times U^2 \quad (4)$$

where F_D represents drag force, which is defined as the force component in the direction of the flow velocity; C_d is the drag coefficient (= 2.0 for a rectangular box); ρ is the mass density of the fluid (= 1,000 kg/m³ for water); A is the reference area (= tsunami height × building width); and U is the flow velocity relative to the object. This simulation calculated the drag force per meter as the building unit width. Therefore, the unit of the drag force is kN/m.

Table 3 demonstrates the relationship between building damage and the required tsunami height and hydrodynamic force based on building damage data from Japan.

Table 3 Relationship between building damage and required tsunami height and hydrodynamic force

Building Composition	Moderate Damage	Major Damage
Wood	1.5 m / 15.6 - 27.4 kN/m	2.0 m / 27.4 - 49.0 kN/m
Reinforced Concrete (RC)	N/A / 61 - 111 kN/m	8.0 m / 332 - 603 kN/m

Figure 11 displays an example of the importance of using hydrodynamic force to assess building damage. The 2011 Great East Japan Tsunami was selected as a representative of a large tsunami event that caused damages over a wide area. This section focuses on damages to reinforced concrete buildings by using major damage criteria of 7 m and 300 kN/m. The simulated maximum tsunami height was clearly higher than 7 m along the Sanriku Ria coast and lower than 7 m along the Sendai Plains coast (Region A). Nevertheless, the maximum simulated hydrodynamic force (higher than 300 kN/m) was found along the shoreline of both areas including Region A where decreased in Region B. Thus, only utilizing only tsunami height could underestimate the degree of building damages.

Figures 12 and 13 show another example with the 1852 Banda Sea Tsunami as a representative of a small tsunami inside a small sea that is surrounded by many small islands. At the deepest part of the bay, the maximum simulated tsunami height and hydrodynamic force were 4.93 m and 77.6 kN/m, respectively. However, the maximum hydrodynamic force (121.15 kN/m) was located at the edge of the bay, where the tsunami height was only 2.69 m. In addition, the tsunami height at the bay entrance was only 1.59 m but the hydrodynamic force was 62.57 kN/m. Thus, wooden houses might be interpreted as having experienced moderate damage when using the tsunami height or major/complete damage when using the hydrodynamic force.

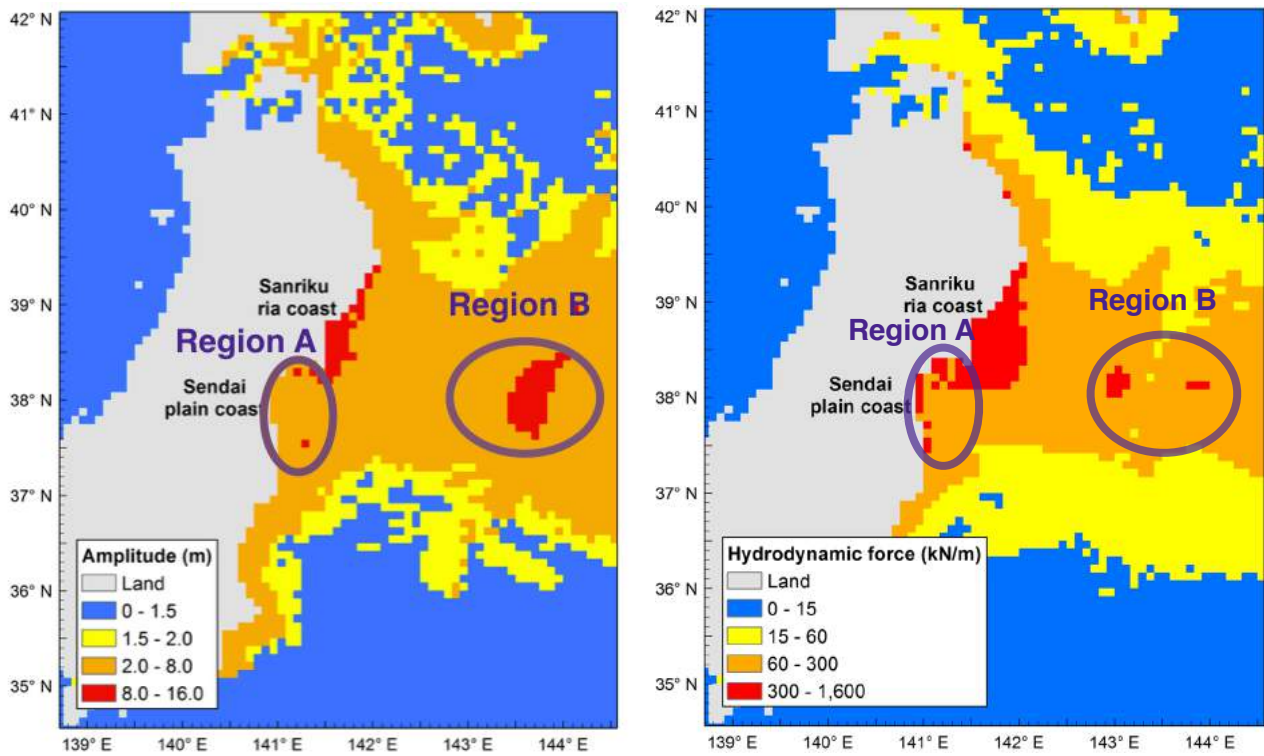


Figure 11

Simulated maximum tsunami height in meters (left) and hydrodynamic force in kN/m (right) for the 2011 Great East Japan tsunami

Note. Higher risk of building damage can be seen in region A when considering the hydrodynamic forces.

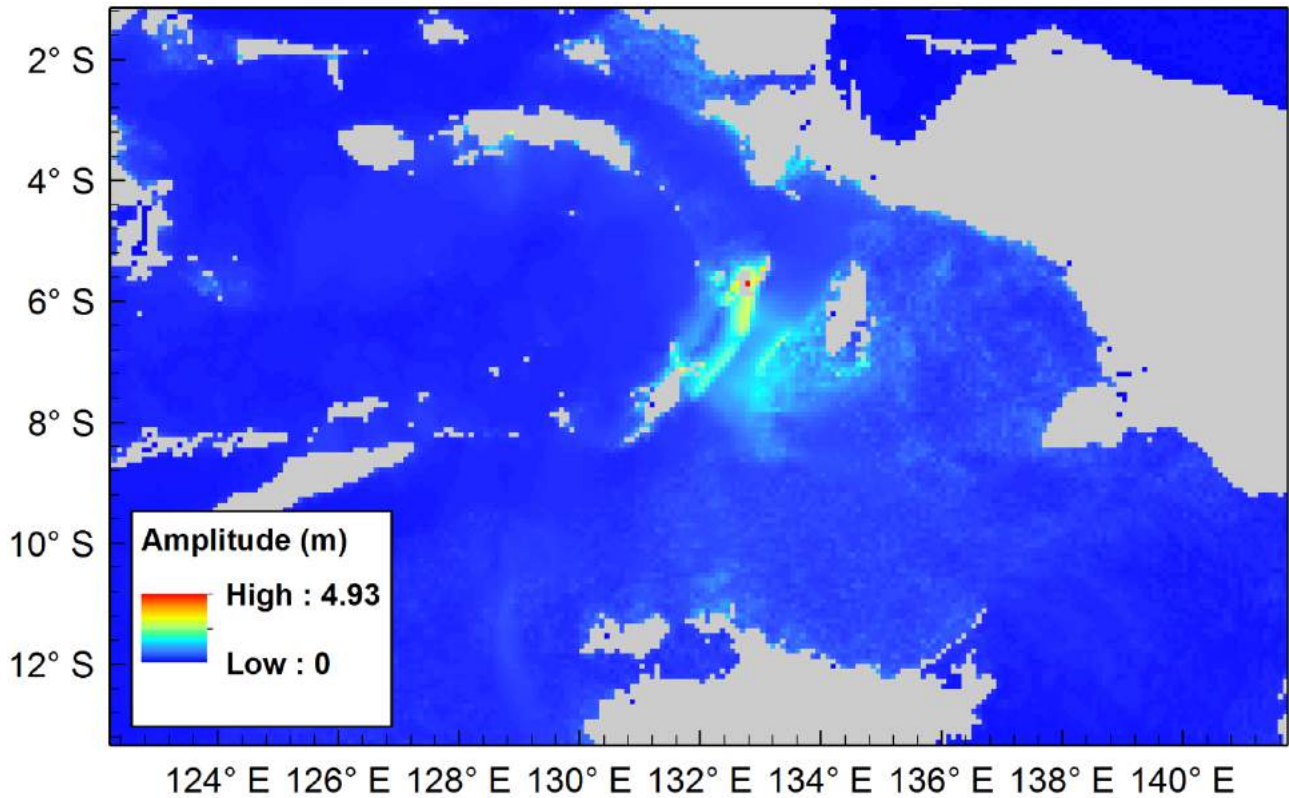


Figure 12

Simulated maximum tsunami height in meters (left) and hydrodynamic force in kN/m (right) for the 1852 Banda Sea tsunami (regional scale)

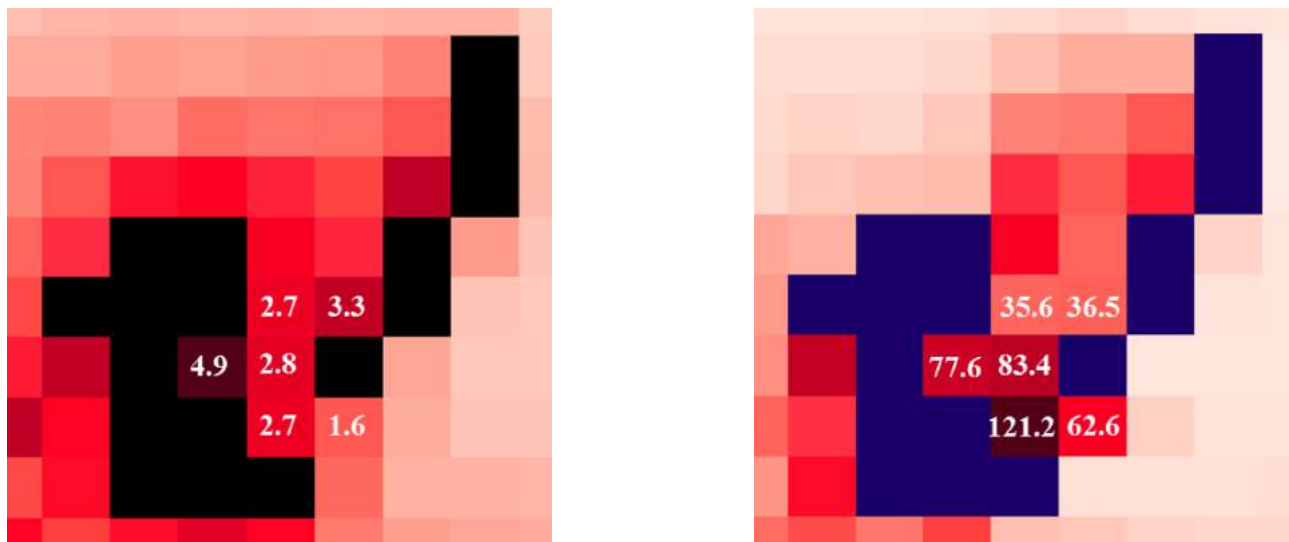


Figure 13

Simulated maximum tsunami height in meters (left) and hydrodynamic force in kN/m (right) for the 1852 Banda Sea tsunami (local scale near the tsunami source)

9.3 Tsunami Traveling Times

It is imperative to determine the arrival time of a tsunami in order to properly evacuate people located in at-risk areas. The arrival time is estimated based on its source location, topography and bathymetry, and its influence on the speed of the waves. **Figure 14** displays tsunami propagation and the travel time of the 2004 Indian Ocean tsunami.

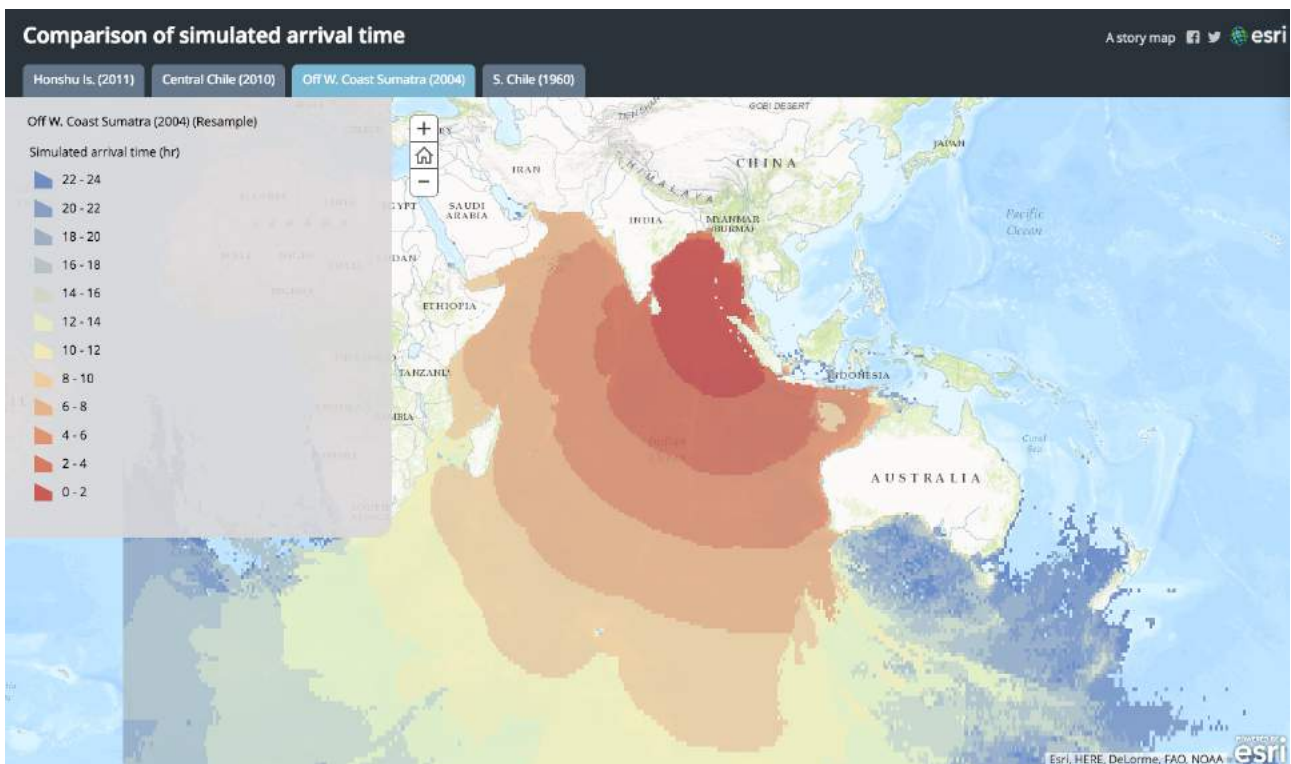


Figure 14

Tsunami arrival time

Note. An example from the 2004 Indian Ocean tsunami

9.4 Importance of assessing historical and future tsunamis in global scale

Simulated maximum tsunami amplitude based on the selected seismic gaps in Pacific Ocean is shown in **Figure 15**. An example of a major tsunami in a large seismic gap is shown for the Aleutian Islands due to its length of 400-500 km. This tsunami can also affect Japan and other countries in Southeast Asia. In terms of tsunami arrival time, New Zealand is a good example regarding the importance of assessing past and future tsunamis on a global scale and raising tsunami awareness in coastal areas. New Zealand was affected by major historical tsunamis from distant earthquakes such as in 1687 (from Peru), 1730 (from central Chile) and 1960 (South Chile). Tsunami arrival time of these tsunamis exceeded 10 hours (**Figure 16** left), however, locally generated tsunamis in the future can arrive New Zealand within an hour (**Figure 16** right). Therefore, it is important to educate and raise coastal residents' awareness that future tsunami characteristics such as its arrival time, may differ from past events.

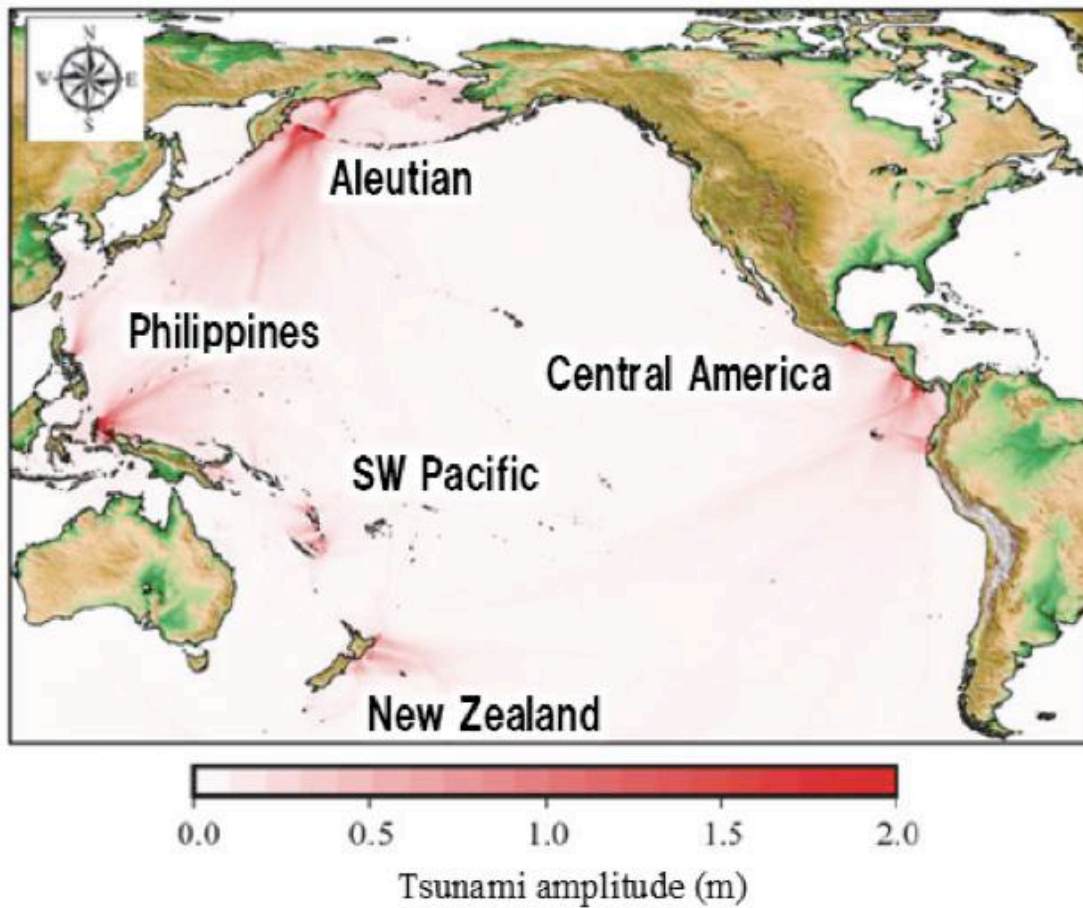


Figure 15
Simulated maximum tsunami amplitude based on the selected seismic gap

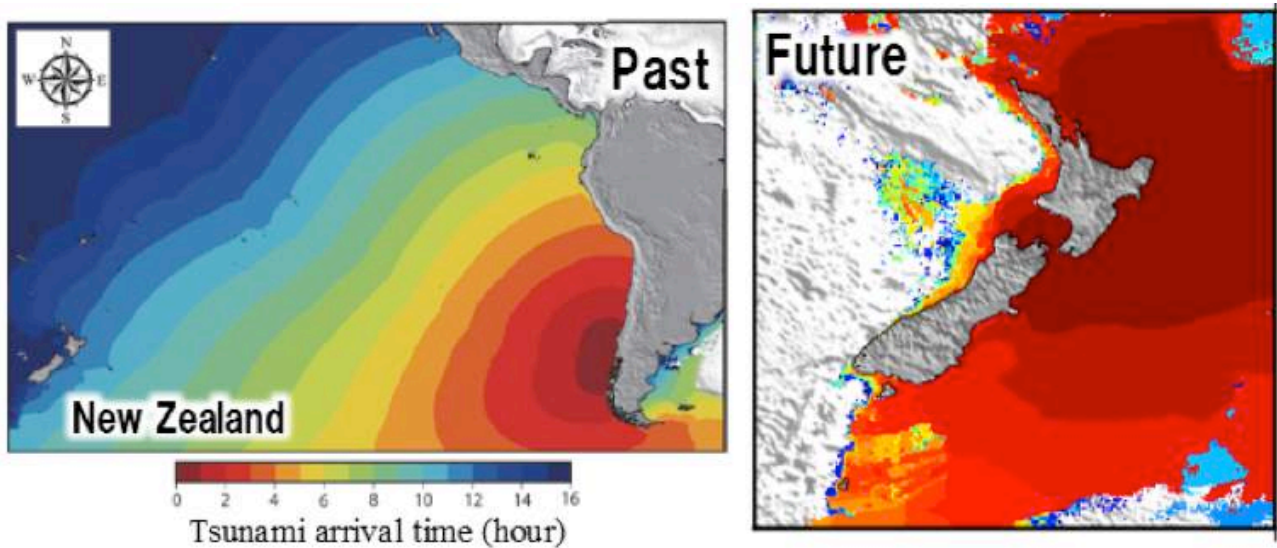


Figure 16
The 1960 Chilean tsunami arrival time (left) and the combined tsunami arrival times of local tsunamis off the coast of New Zealand

10. Conclusions

- A global tsunami assessment has been developed based on select 103 tsunamis generated by major historical earthquakes and 18 major potential tsunamis generated by earthquakes in seismic gaps
- This observation demonstrates the importance of assessing or understanding the hazards based on historical events beyond recent experiences
- Comparisons between tsunami height and wave force demonstrate that only using the tsunami height might underestimate the extent of building damage
- Tsunami arrival time or other tsunami characteristics of the potential tsunamis can differ from what happened in the past
- This report can contribute as supplementary information for policy makers, urban planners, engineers, as well as scholarly research

**WORLD
TSUNAMI
AWARENESS
DAY**
5 NOVEMBER
2017



“We wish that as a part of World Tsunami Awareness Day, the results of our research will contribute to increasing tsunami awareness at the global scale, especially in comparatively low tsunami risk areas, and reduce human loss from tsunamis in the future.”

11. References

- Atwater, B. F., Musumi-Rokkaku, S., Satake, K., Tsuji, Y., Ueda, K., & Yamaguchi, D. K. (2015). *The orphan tsunami of 1700-Japanese clues to a parent earthquake in North America* (2nd ed.). Seattle, University of Washington Press, U.S. Geological Survey Professional Paper 1707.
- Dziewonski, A. M., Chou, T. A., & Woodhouse, J. H. (1981). Determination of earthquake source parameters from waveform data for studies of global and regional seismicity. *Journal of Geophysical Research: Solid Earth*, 86(B4), 2825-2852. doi: 10.1029/JB086iB04p02825
- Fujii, Y., & Satake, K. (2013). Slip distribution and seismic moment of the 2010 and 1960 Chilean earthquakes inferred from tsunami waveforms and coastal geodetic data. *Pure and Applied Geophysics*, 170(9), 1493-1509. doi: 10.1007/s00024-012-0524-2
- General Bathymetric Chart of the Oceans (GEBCO) (2016). *Gridded bathymetry data*. Retrieved Aug. 6, 2016, from http://www.gebco.net/data_and_products/gridded_bathymetry_data
- Ichinose, G., Somerville, P., Thio, H. K., Graves, R., & O'Connell, D. (2007). Rupture process of the 1964 Prince William Sound, Alaska, earthquake from the combined inversion of seismic, tsunami, and geodetic data. *Journal of Geophysical Research*, 112(B7), B07306. doi: 10.1029/2006JB004728
- Imamura, F. (1996). Simulation of wave-packet propagation along sloping beach by TUNAMI-code. In H. Yeh, P. Liu, & C. Synolakis (Eds.), *Long-wave Sunup Models* (pp. 231-241), Singapore: World Scientific.
- Imamura, F., Yalciner, A. C., & Ozyurt, G. (2006). *Tsunami Modelling Manual (TUNAMI model)*. Miyagi: Tsunami Engineering Laboratory, Tohoku University.
- IUGG/IOC TIME Project. (1997). IUGG/IOC TIME Project: Numerical method of tsunami simulation with the leap-frog scheme. *Intergovernmental Oceanographic Commission Manuals and Guides*, 35. Geneva: UNESCO.
- Johnson, J. M., & Satake, K. (1999). Asperity distribution of the 1952 Great Kamchatka earthquake and its relation to future earthquake potential in Kamchatka. *Pure and Applied Geophysics*, 154(3), 541-553. doi: 10.1007/s000240050243
- Lay, T., Kanamori, H., Ruff, L. (1982). The Asperity and the Nature of Large Subduction Zone Earthquakes. *Earthquake Prediction Research*, 1(1), 3-71.
- Leelawat, N., Suppasri, A., & Imamura, F. (2015). The tsunami warning system in Thailand: A part of the reconstruction process after the 2004 Indian Ocean Tsunami. In V. Santiago-Fandiño, Y. A. Kontar, & Y. Kaneda (Eds.), *Advances in Natural and Technological Hazards Research: Vol. 44. Post-Tsunami Hazard: Reconstruction and Restoration* (pp. 111-119), Cham: Springer International Publishing. doi: 10.1007/978-3-319-10202-3_8
- Løvholt, F., Glimsdal, S., Harbitz, C. B., Zamora, N., Nadim, F., Peduzzi, P., Dao, H., & Smebye, H. (2012). Tsunami hazard and exposure on the global scale. *Earth-Science Reviews* 110(1), 58-73. doi: 10.1016/j.earscirev.2011.10.002
- Nagano, O., Imamura, F., & Shuto, N. (1991). A numerical model for a far-field tsunamis and its application to predict damages done to aquaculture. *Natural Hazards* 4(2). 235-255. doi: 10.1007/BF00162790
- National Geophysical Data Center / World Data Service (NGDC/WDS). (2015). *Global Historical Tsunami Database*. National Geophysical Data Center, NOAA. Retrieved Sep. 21, 2016, from doi: 10.7289/V5PN93H7
- National Oceanic and Atmospheric Administration (NOAA). (2016). *Hokkaido Nansei-Oki Tsunami, July 12, 1993*. Retrieved October 27, 2016, from <https://catalog.data.gov/dataset/hokkaido-nansei-oki-tsunami-july-12-1993>

- Okada, Y. (1985). Surface deformation due to shear and tensile faults in a half-space. *Bulletin of the Seismological Society of America*, 75(4), 1135-1154.
- Okal, E. A., Synolakis, C. E., Uslu, B., Kalligeris, N. and Voukouvalas, E. (2009) The 1956 earthquake and tsunami in Amorgos, Greece, *Geophysical Journal International*. 178(3), 1533-1554. doi: 10.1111/j.1365-246X.2009.04237.x
- Papadopoulos G. A., & Imamura, F. (2001). A proposal for a new tsunami intensity scale. *Proceedings of the International Tsunami Symposium, Session: 5, No. 5-1* (pp. 569-577), Seattle, WA.
- Papazachos B. C., Scordilis, E. M., Panagiotopoulos, D. G., Papazachos, C. B., & Karakaisis, G. F. (2004). Global relations between seismic fault parameters and moment magnitude of earthquakes. In *Bulletin of the Geological Society of Greece, Vol: 36, No: 3, Proceedings of the 10th International Congress* (pp. 1482-1489), Thessaloniki, Greek.
- Pacific Tsunami Warning Center. (2016). *Frequently Asked Questions (FAQ)*. Retrieved October 27, 2016, from <http://www.tsunami-alarm-system.com/en/phenomenon-tsunami/occurrences-atlantic-ocean.html>
- Piatanesei, A., & Tinti, S. (2002). Numerical modelling of the September 8, 1905 Calabrian (southern Italy) tsunami. *Geophysical Journal International*, 150(1), 271-284. doi: 10.1046/j.1365-246X.2002.01700.x
- Santos, A., Koshimura, S., & Imamura, F. (2009). The 1755 Lisbon tsunami: Tsunami source determination and its validation. *Journal of Disaster Research*, 4(1), 41-52. doi: 10.20965/jdr.2009.p0041
- Suppasri, A., Goto, K., Muhari, A., Ranasinghe, P., Riyaz, M., Affan, M., Mas, E., Yasuda, M., & Imamura, F. (2015). A decade after the 2004 Indian Ocean tsunami- The progress in disaster preparedness and future challenges in Indonesia, Sri Lanka, Thailand and the Maldives. *Pure and Applied Geophysics*, 172(12), 3313-3341. doi: 10.1007/s00024-015-1134-6
- Suppasri, A., Imamura, F., & Koshimura, S. (2010). Effects of the rupture velocity of fault motion, ocean current and initial sea level on the transoceanic propagation of tsunami. *Coastal Engineering Journal*, 52(2), 107-132. doi: 10.1142/S0578563410002142
- Suppasri, A., Koshimura, S., & Imamura, F. (2011). Developing tsunami fragility curves based on the satellite remote sensing and the numerical modeling of the 2004 Indian Ocean tsunami in Thailand. *Natural Hazards and Earth System Sciences*, 11(1), 173-189. doi: 10.5194/nhess-11-173-2011
- Suppasri, A., Koshimura, S., Imai, K., Mas, E., Gokon, H., Muhari, A., & Imamura, F. (2012). Damage characteristic and field survey of the 2011 Great East Japan tsunami in Miyagi prefecture. *Coastal Engineering Journal*, 54(1), 1250008. doi: 10.1142/S0578563412500052
- Suppasri, A., Latcharote, P., Bricker, J. D., Leelawat, N., Hayashi, A., Yamashita, K., Makinoshima, F., Roeber, V., & Imamura, F. (2016). Improvement of tsunami countermeasures based on lessons from the 2011 great east japan earthquake and tsunami -Situation after five years-. *Coastal Engineering Journal*, 58(4), 1640011. doi: 10.1142/S0578563416400118
- Suppasri, A., Leelawat, N., Latcharote, P., Roeber, V., Yamashita, K., Hayashi, A., Ohira, H., Fukui, K., Hisamatsu, A., Nguyen, D., & Imamura, F. (2017). The 2016 Fukushima earthquake and tsunami: Local tsunami behavior and recommendations for tsunami disaster risk reduction. *International Journal of Disaster Risk Reduction*, 21, 323-330. doi: 10.1016/j.ijdr.2016.12.016
- Tsunami Alarm System. (2016a). *Occurrences of Tsunamis in the Atlantic Ocean*. Retrieved October 27, 2016, from <http://www.tsunami-alarm-system.com/en/phenomenon-tsunami/occurrences-atlantic-ocean.html>
- Tsunami Alarm System. (2016b). *Occurrences of Tsunamis in the Mediterranean*. Retrieved October 27, 2016, from <http://www.tsunami-alarm-system.com/en/phenomenon-tsunami/occurrences-mediterranean.html>
- Tsunami Laboratory. (2016). *Analysis of the Tsunami Travel Time maps for damaging tsunamis in the World Ocean*. Retrieved October 27, 2016, from http://tsun.sccc.ru/TTT_rep.htm

United Nations International Strategy for Disaster Reduction (UNISDR). (2009). *Global Assessment Report 2009, Risk and poverty in a changing climate, Invest today for a safer tomorrow*. Retrieved Oct. 13, 2016, from <http://www.preventionweb.net/english/hyogo/gar/2009/?pid:34&pif:3>

U.S. Geological Survey (USGS). (2016). *Earthquake Glossary - seismic gap*. Retrieved October 27, 2016, from <http://www.tsunami-alarm-system.com/en/phenomenon-tsunami/occurrences-mediterranean.html>

Wang, D., & Becker, N. (2015). *Tsunami forecast model animation of the 1 November 1755 Lisbon, Portugal tsunami*. Retrieved October 27, 2016, from <https://www.youtube.com/watch?v=7DpF38OKYz0>

Contact

IRIDeS, Tohoku University

email Professor Dr. Fumihiko Imamura
imamura@irides.tohoku.ac.jp

Associate Professor Dr. Anawat Suppasri
suppasri@irides.tohoku.ac.jp

Dr. Panon Latcharote
panon@irides.tohoku.ac.jp

Mr. Takuro Otake
takuro.ohtake.q2@dc.tohoku.ac.jp

Dr. Natt Leelawat (Chulalongkorn University, Thailand)
natt.l@chula.ac.th

Dr. David N. Nguyen (The University of Tokyo, Japan)
davidn@s.k.u-tokyo.ac.jp

Postal Address International Research Institute of Disaster Science (IRIDeS)
Tohoku University
468-1 Aramaki-Aza Aoba, Aoba-ku
Sendai 980-0845 Japan

Phone +81-22-752-2092

Fax +81-22-752-2091

URL <http://irides.tohoku.ac.jp/>

Download the latest version of this report at
[http://irides.tohoku.ac.jp/project/
global_assessment_tsunami_hazards.html](http://irides.tohoku.ac.jp/project/global_assessment_tsunami_hazards.html)



**WORLD
TSUNAMI
AWARENESS
5 NOVEMBER
2017 DAY**

